JOURNAL OF GEOPHYSICAL RESEARCH, VOL. 92, NO. A7, PAGES 7341–7353, JULY 1, 1987

Electron Impact Ionization in the Vicinity of Comets

T. E. CRAVENS, J. U. KOZYRA, A. F. NAGY, T. I. GOMBOSI,[1] AND M. KURTZ

Space Physics Research Laboratory, University of Michigan, Ann Arbor

The solar wind interacts very strongly with the extensive cometary coma, and the various interaction processes are initiated by the ionization of cometary neutrals. The main ionization mechanism far outside the cometary bow shock is photoionization by solar extreme ultraviolet radiation. Electron distributions measured in the vicinity of comets Halley and Giacobini-Zinner by instruments on the VEGA and ICE spacecraft, respectively, are used to calculate electron impact ionization frequencies. Ionization by electrons is of comparable importance to photoionization in the magnetosheaths of Comets Halley and Giacobini-Zinner. The ionization frequency in the inner part (radial distance $\approx 10^4$ km) of the cometary plasma region of comet Halley is several times greater than the photoionization value. Tables of ionization frequencies as functions of electron temperature are presented for H_2O, CO_2, CO, O, N_2, and H.

1. INTRODUCTION

Ionization of neutral atoms and molecules in the extensive coma surrounding a comet produces heavy ions which contaminate and mass load the solar wind [cf. *Mendis et al.*, 1985]. These heavy ions (e.g., H_2O^+, OH^+, O^+, CO^+, etc.) are initially at rest but are picked up by the solar wind in a highly anisotropic manner [cf. *Ip and Axford*, 1982; *Galeev et al.*, 1985; *Cravens*, 1986*b*], which results in wave growth and the development of magnetic turbulence [*Winske et al.*, 1985; *Sagdeev et al.*, 1986; *Smith et al.*, 1986; *Tsurutani and Smith*, 1986; *Riedler et al.*, 1986]. These pick-up ions were observed to be largely isotropized near comets Giacobini-Zinner (G/Z) and Halley, as would be expected, due to the magnetic fluctuations [*Hynds et al.*, 1986; *Ipavich et al.*, 1986; *Gloeckler et al.*, 1986; *Somogyi et al.*, 1986; *McKenna-Lawlor*, 1986]. The long cometary plasma tails are another manifestation of mass loading of the solar wind by ionized cometary neutrals [*Brandt*, 1982].

The solar wind cometary interaction process is initiated by the ionization of cometary neutrals. Photoionization of these neutrals by solar extreme ultraviolet radiation (EUV) has been assumed to be the main source of ionization near comets [cf. *Mendis et al.*, 1985], although both charge exchange with solar wind protons (not a net ionization source but still a source of heavy ions) and electron impact ionization have also been suggested [*Wallis*, 1973]. There are indications that some ionization source in excess of photoionization is indeed required in the cometary plasma environment (see reviews by *Ip and Axford* [1982] and *Mendis et al.* [1985]). *Boice et al.* [1986] included electron impact ionization in their ionospheric/hydrodynamic model and *Körösmezey et al.* [1987] included secondary ionization from photoelectrons in their ionospheric model. *Ip* [1986] and *Cravens* [1986*a*] also discussed the importance of electron impact ionization. One possibility that has been suggested is the critical velocity ionization mechanism in which some of the energy of a plasma flowing with sufficient bulk velocity is imparted to the electrons [*Alfvén*, 1954; *Formisano et al.*, 1982; *Haerendel*, 1986]. The electrons, if they have been sufficiently heated, can then ionize the background neutrals.

The purpose of this paper is to assess quantitatively the importance of electron impact ionization in various regions of the cometary plasma environment and compare this ionization source with the photoionization source. Electron energy distribution functions have been measured in the vicinity of comet G/Z [*Bame et al.*, 1986] and comet Halley [*Gringauz et al.*, 1986*a*, *b*]. We have calculated ionization frequencies and rates using electron impact ionization cross sections found in the literature and published electron spectra from the International Cometary Exploration (ICE) mission to comet G/Z and from the VEGA mission to comet Halley. We also present, in the form of both tables and graphs, the results of calculations of ionization frequencies for Maxwellian distributions of electrons for a range of temperatures and for a variety of neutral "targets" (i.e., H_2O, O, H, CO_2, CO, N_2). These tables are used to calculate the electron impact ionization rate along the ICE trajectory near the tail of comet G/Z using the results of *Zwickl et al.* [1986], who fit measured electron spectra with three Maxwellian distributions (low-, mid-, and high-temperature components). Finally, some of the implications of the calculated ionization rates are discussed including the concept of plasma mantle and its relation to the Venus plasma mantle [*Verigin et al.*, 1978; *Spenner et al.*, 1980; *Vaisberg and Zeleny*, 1984] and to the cometary plasma region [*Gringauz et al.*, 1986*a*, *b*].

2. REVIEW OF THE PHOTOIONIZATION PROCESS

Solar EUV photons with energies in excess of the ionization potential I_{sk} (for species s and final ion state k) of a given neutral species M can photoionize the molecules (or atoms) of that species:

$$h\nu + M \rightarrow M^+ + e \qquad (1)$$

The resulting photoelectron carries off energy $E = h\nu - I_{sk}$. The photoion M^+ may end up either in the ground state or an excited final state, and the ionization potential for a particular species and ion final state reflects this. *Banks and Kockarts* [1973], *Gombosi et al.* [1986], and *Huebner* [1985] discuss this process, and Gombosi et al. presented tables of solar EUV fluxes for 32 wavelength intervals as well as photoaborption and photoionization cross sections for H_2O. *Körösmezey et al.* [1987] calculated photoionization frequencies for H_2O for both solar minimum and maximum conditions using the tables from *Gombosi et al.* [1986]. All these numbers assume a heliocentric distance of 1 AU. These ionization frequencies are reproduced here in Table 1, and they will serve as a standard

[1]Also at Central Research Institute for Physics, Budapest, Hungary.

Paper number 6A8761.
0148-0227/87/006A-8761$05.00

TABLE 1. Photoionization Frequencies at 1 AU

Solar Cycle Conditions	$H_2O \rightarrow H_2O^+$	$H_2O \rightarrow OH^+$	$H_2O \rightarrow H^+$	CO_2^+	CO^+	O^+	N_2^+	H^+	OH^+
Maximum	8.70(−7)	1.57(−7)	2.19(−8)	1.77(−6)	1.12(−6)	7.01(−7)	8.82(−7)	9.6(−8)	2–3.5(−7)
Minimum	3.19(−7)	5.48(−8)	7.31(−9)	6.04(−7)	3.87(−7)	2.38(−7)	3.06(−7)	5.5(−8)	

Units s^{-1}. The information for CO_2^+, CO^+, O^+, and N_2^+ was taken from *Torr and Torr* [1985], for H^+ from *Huebner* [1985], and for OH^+ from *Wallis* [1973]. When the product ion is not the same as the parent neutral molecule, it is so indicated. Read 8.70(−7) as 8.70×10^{-7}.

of comparison for the electron impact ionization frequencies presented later.

The photoionization frequencies for O at solar minimum and solar maximum are 2.4×10^{-7} s^{-1} and 7×10^{-7} s^{-1}, respectively, and for H are 5.5×10^{-8} s^{-1} and 9.6×10^{-8} s^{-1}, respectively [*Banks and Kockarts*, 1973; *Huebner*, 1985]. The frequencies for OH are in the range 2–3.5 $\times 10^{-7}$ s^{-1} [cf. *Wallis*, 1973].

3. Review of the Charge Exchange Process

The charge exchange, or transfer, process is not a net source of ionization in that electrons are not produced. However, the charge exchange of solar wind protons with heavy cometary neutrals (species M) does contribute, in the same manner as photoionization, to the contamination and mass loading of the solar wind [*Wallis*, 1973]:

$$H^+ + M \rightarrow H + M^+ \tag{2}$$

Charge exchange of solar wind protons with cometary H in the supersonic solar wind does not "mass load" the flow but does affect the dynamics by heating the plasma; the picked-up H^+ ions initially move in cycloidal trajectories and are hotter than the solar wind protons that they have replaced. On the other hand, in the shocked, subsonic solar wind this same process cools the plasma since the replacement protons are slower than the shocked solar wind protons. Similarly, charge transfer of heavy pick-up ions with cometary neutrals in shocked subsonic solar wind cools the plasma and therefore has dynamical effects [*Galeev et al.*, 1985].

Wallis [1973] estimated charge transfer rates (frequencies) for typical solar wind conditions with an average flux of $\langle nv \rangle = 3 \times 10^8$ cm^{-2} s^{-1}. We estimate very similar charge transfer rates which are shown in Table 2 and are all roughly 5×10^{-7} s^{-1}, which is comparable to typical photoionization frequencies for 1 AU at solar minimum. However, for solar maximum, photoionization rates are considerably larger than charge transfer rates for typical solar wind parameters.

TABLE 2. Charge Exchange

Species	Cross Section, cm^2	Source	Frequency,* s^{-1}
H	2×10^{-15}	cf. *Mott and Massey* [1965]	6×10^{-7}
O	8×10^{-16}	*Stebbings et al.* [1964]	2.4×10^{-7}
H_2O	1.9×10^{-15}	*Tawara* [1978]	5.7×10^{-7}
CO_2	$\approx 2 \times 10^{-15}$	estimate	$\approx 6 \times 10^{-7}$
OH	$\approx 3 \times 10^{-15}$	cf. *Wallis* [1973]	$\approx 9 \times 10^{-7}$

Solar wind speed $V = 400$ km/s; $\langle nv \rangle = 3 \times 10^8$ s^{-1} solar wind proton flux.

*Frequency $\cong \langle nv \rangle \sigma$.

4. Electron Impact Ionization Cross Sections

The electron impact ionization process for species M can be represented as

$$e + M \rightarrow M^+ + e + e \tag{3}$$

where the energy of the incident electron must exceed the ionization potential I_{sk}. The secondary electrons generated by this process have energies equal to the incident energy minus the ionization potential, and these electrons (as well as tertiary electrons) can also ionize neutrals if they are sufficiently energetic. The ionization cross sections and the branching ratios for the ion final states used in this paper for H_2O, O, H, CO_2, CO, and N_2 were taken from the references listed in Table 3*a*. References to the original experimental data can be found in these references. Total ionization cross sections are plotted versus incident electron energy in Figure 1. Table 3*b* lists the ionization potentials for various ion final states.

5. Electron Impact Ionization Frequencies for Maxwellian Electron Distributions

Assume that the electron distribution function is isotropic and is given by $n_e f(v)$, where n_e is the total electron density; f is normalized to unity, and v is the electron velocity. The ionization frequency R_{sk} (for species s and ion final state k) can be calculated from the following integral:

$$R_{sk} = n_e \int_{v_{sk}}^{\infty} v \sigma_{sk}(v) f(v) 4\pi v^2 \, dv \tag{4}$$

where v_{sk} is the velocity corresponding to I_{sk} and σ_{sk} is the relevant cross section. The ionization rate R_{sk}* is found by multiplying R_{sk} by the density n_s of the neutral species s.

In general, the electron distribution function is not Maxwellian; however, it can sometimes be approximated with one or more Maxwellians. We have numerically evaluated the integral in equation (4) for several neutral species and for many ion final states using the Maxwellian distribution function for temperature T_e:

$$f(v) = [m_e/2\pi k_B T_e]^{3/2} \exp\{-m_e v^2/2k_B T_e\} \tag{5}$$

where m_e is the electron mass and k_B is Boltzmann's constant. Tabulations of ionization frequencies for $n_e = 1$ (or, equivalently, R_{sk}/n_e) are provided in Tables 4*a*–4*f*. Values of R_s/n_e for total ionization (summed over all ion final states k) are plotted versus T_e (Figure 2).

The electron density and temperature in the unperturbed solar wind are typically about 5 cm^{-3} and 1.5×10^5 K, respectively [*Feldman et al.*, 1975], giving a typical ionization frequency for H_2O (see Table 4 or Figure 2) of 8×10^{-8} s^{-1}. This value is less than 20% of typical photoionization values even for solar minimum. However, solar wind electrons are heated downstream of shocks. For example, a typical effective

TABLE 3a. Cross-Section References

Cross Section	Reference
CO_2	*Sawada et al.* [1972*a*]
CO	*Sawada et al.* [1972*b*]
H_2O	*Olivero et al.* [1972]
O	*Green and Stolarski* [1972]
N_2	*Green and Stolarski* [1972]
H	*Banks and Kockarts* [1973]

temperature behind an interplanetary shock (or a cometary shock, as will be alluded to later) is about 3×10^5 K, giving an ionization frequency of 2.1×10^{-7} s^{-1}, which is about 50% of the photoionization value for solar minimum. Behind a stronger shock, like the Venus bow shock, densities and temperatures can reach approximately 30 cm^{-3} and 10^6 K, respectively, giving values of R_s for CO_2 and O of 5×10^{-6} s^{-1} and 2×10^{-6} s^{-1}, respectively. These ionization frequencies are considerably larger than either photoionization or charge transfer values, even for solar maximum conditions.

6. Electron Impact Ionization Rates From Measured Electron Distributions

Solar Wind and Magnetosheath Regions

Electrons in the unperturbed solar wind generally appear Maxwellian with temperatures of about 10^5 K, whereas behind collisionless shocks, including interplanetary shocks, electron distributions usually appear to be "flat-topped" with much higher effective temperatures [*Feldman et al.*, 1975]. Experimenters have found the following expression useful for describing these distribution functions:

$$f(v) = f_0 \exp\{-(v/v_0)^p\} \quad (6)$$

TABLE 3b. Ionization Potentials I_{sk}

Final State	Ionization Potential, eV
Water	
$H_2O^+(X)$	12.62
$H_2O^+(A)$	13.2
OH^+	18.
O^+	18.6
H^+	18.7
Carbon dioxide	
$CO_2^+(X)$	13.76
$CO_2^+(A)$	17.8
$CO_2^+(B)$	18.1
$CO_2^+(C)$	19.4
Dissociated	36.0
Carbon monoxide	
$CO^+(X)$	14.01
$CO^+(A)$	16.5
$CO^+(B)$	19.7
Dissociated	22.0
Molecular nitrogen	
$N_2^+(X)$	15.58
$N_2^+(A)$	16.7
$N_2^+(B)$	18.8
$N_2^+(C)$	23.6
$N_2^+(D)$	≈22.0
40 eV	40.0
Atomic oxygen	
$O^+(^4S)$	13.62
$O^+(^2D)$	16.9
$O^+(^2P)$	18.6
Atomic hydrogen	13.6

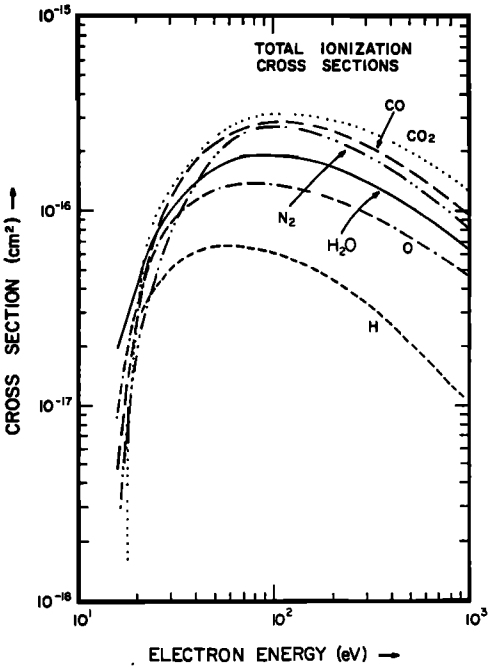

Fig. 1. Electron impact total ionization cross sections as a function of electron energy for several species. Source references are provided in Table 3a.

where v_0 is a characteristic velocity and p is an index which is 2 for Maxwellians and is typically about 3–4 for shocked electrons [*Feldman et al.*, 1975; *Thomsen et al.*, 1986].

The electron distributions observed behind the cometary bow shock (or bow wave) of comet G/Z appear to be similar to those observed behind other shocks in the solar system, although the cometary shocks at Halley and G/Z are very broad, weak, and turbulent [*Neubauer et al.*, 1986; *Riedler et al.*, 1986; *Gringauz et al.*, 1986*a*, *b*; *Smith et al.*, 1986; *Thomsen et al.*, 1986; *Jones et al.*, 1986], as was largely anticipated prior to the cometary missions [e.g., *Schmidt and Wegmann*, 1982; *Galeev and Lipatov*, 1984; *Galeev et al.*, 1985; *Omidi et al.*, 1986]. The electron distributions upstream of the G/Z bow wave have values of p very close to 2 with effective temperatures of about 2×10^5 K, whereas downstream of the shock (or interaction region) in the magnetosheath, $p \approx 3.5$ with effective temperatures more like 4×10^5 K [*Bame et al.*, 1986; *Thomsen et al.*, 1986]. *Thomsen et al.* [1986] demonstrated that within the interaction region, both types of electron distributions were present at different times. The early results from the electron spectrometer on the VEGA spacecraft indicate that the situation at comet Halley is similar to G/Z, both upstream and downstream of the bow shock [*Gringauz et al.*, 1986*a*, *b*]. Similar results were obtained by the electron spectrometer on the Giotto spacecraft [*Rème et al.*, 1986]. Figure 3*a* reproduces a published VEGA 2 electron spectrum for the solar wind far from the comet.

We have calculated total ionization frequencies for H_2O and O (that is, R_{H_2O} and R_O) with equation (4) using several measured (by the plasma instruments on ICE) solar wind electron distributions, including two upstream spectra and one magnetosheath spectrum. We also calculated ionization frequencies for the VEGA solar wind spectrum shown in Figure 3*a*. These calculated ionization frequencies (and references for the spectra) are given in Table 5. The ionization frequencies are about 2×10^{-7} s^{-1} for all the upstream solar wind elec-

TABLE 4a. Ionization Frequencies per Electron for Impact Ionization of Water by Maxwellian Electrons

Temp. (K)	H2O+	OH+	H+	O+	H2+	Total
1.000E+04	2.168E-15	1.561E-19	6.878E-20	6.298E-21	9.598E-23	2.188E-15
2.000E+04	5.154E-12	2.584E-14	1.368E-14	1.381E-17	8.877E-17	5.195E-12
3.000E+04	7.791E-11	1.597E-12	9.332E-13	9.758E-14	9.566E-15	8.055E-11
4.000E+04	3.231E-10	1.331E-11	8.333E-12	8.861E-13	1.042E-13	3.457E-10
5.000E+04	7.878E-10	4.919E-11	3.244E-11	3.480E-12	4.490E-13	8.734E-10
6.000E+04	1.463E-09	1.202E-10	8.262E-11	8.904E-12	1.209E-12	1.676E-09
7.000E+04	2.314E-09	2.311E-10	1.643E-10	1.775E-11	2.481E-12	2.730E-09
8.000E+04	3.303E-09	3.814E-10	2.791E-10	3.018E-11	4.289E-12	3.998E-09
9.000E+04	4.396E-09	5.677E-10	4.257E-10	4.602E-11	6.601E-12	5.442E-09
1.000E+05	5.564E-09	7.852E-10	6.015E-10	6.497E-11	9.359E-12	7.025E-09
1.500E+05	1.184E-08	2.174E-09	1.797E-09	1.925E-10	2.744E-11	1.603E-08
2.000E+05	1.800E-08	3.752E-09	3.254E-09	3.453E-10	4.798E-11	2.540E-08
3.000E+05	2.859E-08	6.737E-09	6.210E-09	6.464E-10	8.538E-11	4.227E-08
4.000E+05	3.690E-08	9.220E-09	8.838E-09	9.048E-10	1.145E-10	5.598E-08
5.000E+05	4.347E-08	1.123E-08	1.107E-08	1.118E-09	1.366E-10	6.702E-08
6.000E+05	4.870E-08	1.287E-08	1.297E-08	1.293E-09	1.534E-10	7.599E-08
7.000E+05	5.299E-08	1.420E-08	1.457E-08	1.437E-09	1.664E-10	8.336E-08
8.000E+05	5.651E-08	1.530E-08	1.595E-08	1.558E-09	1.765E-10	8.949E-08
9.000E+05	5.945E-08	1.623E-08	1.713E-08	1.659E-09	1.845E-10	9.465E-08
1.000E+06	6.192E-08	1.700E-08	1.815E-08	1.745E-09	1.908E-10	9.901E-08
1.500E+06	6.977E-08	1.948E-08	2.167E-08	2.021E-09	2.079E-10	1.131E-07
2.000E+06	7.351E-08	2.066E-08	2.359E-08	2.155E-09	2.192E-10	1.201E-07
3.000E+06	7.579E-08	2.141E-08	2.528E-08	2.245E-09	2.106E-10	1.249E-07
4.000E+06	7.517E-08	2.127E-08	2.567E-08	2.237E-09	2.031E-10	1.246E-07
5.000E+06	7.353E-08	2.081E-08	2.552E-08	2.192E-09	1.943E-10	1.222E-07
7.000E+06	6.987E-08	1.977E-08	2.478E-08	2.085E-09	1.790E-10	1.167E-07
1.000E+07	6.473E-08	1.828E-08	2.339E-08	1.931E-09	1.608E-10	1.085E-07

Units of $cm^3\ s^{-1}$. Read 1.000E + 04 as 1.000×10^4. Rows refer to electron temperature, and columns refer to the ion final state. The total ionization frequency for a species is given in the last column.

tron spectra or about 50% of the photoionization frequencies. However, R_{H_2O} and R_O for the ICE magnetosheath spectrum are both about $1 \times 10^{-6}\ s^{-1}$, which is 2–3 times greater than photoionization values.

Ionization frequencies which were calculated using the Maxwellian values from Table 4 are also listed in Table 5 (and are shown in parentheses). For the ICE data, electron densities and temperatures were taken from the relevant references, and for the VEGA spectrum we calculated our own moments of the electron distribution function. The ionization frequencies calculated using the tables are typically about 10–20% smaller than those calculated more accurately using equation (4). The agreement is very good considering the fact that the actual distributions are neither entirely Maxwellian nor isotropic.

Cometary Plasma Region and Plasma Tail Region

Theoretical studies prior to the recent spacecraft cometary encounters predicted that behind the shock the solar wind flow continues to be mass loaded and to slow down, and, finally, to stagnate near the nucleus (see reviews by *Ip and Axford* [1982] and *Mendis et al.* [1985]). One consequence of this slowing down is the buildup of a magnetic barrier and the development of the tailward extension of this barrier, the magnetotail. The VEGA, Giotto, and Suisei missions to comet Halley have confirmed the overall picture in the barrier/stagnation (or cometary plasma region, as it is called by *Gringauz et al.* [1986*a*, *b*]), and the ICE mission has supported this picture in the near-tail region of comet Giacobini-Zinner [cf. *Smith et al.*, 1986; *Slavin et al.*, 1986; *Bame et al.*, 1986].

Not surprisingly, the electron distributions in the stagnation/tail regions are different from those in the solar wind or in the magnetosheath proper. Figure 3*b* reproduces a published [*Gringauz et al.*, 1986*a*] electron spectrum measured by the PLASMAG instrument on the VEGA 2 spacecraft at a UT almost at closest approach to the nucleus of comet Halley (a distance from the nucleus of $r \approx 1.5 \times 10^4$ km). The plasma in this region is stagnated, and its composition is almost entirely cometary; *Gringauz et al.* [1986*a*, *b*] called this the cometary plasma region. The electron flux is significantly enchanced over solar wind values at all energies, and there is a noticeable peak in the spectrum at about 1 keV. We caution the reader that this spectrum (and others taken near closest approach) is potentially "contaminated" and might contain significant errors (M. I. Verigin, private communication, 1986). The electron spectrometer on Giotto did not observe such enhanced electron fluxes [*Rème et al.*, 1986].

The electron distributions in the near-tail of comet G/Z also differ from solar wind or magnetosheath distributions [*Bame et al.*, 1986; *Zwickl et al.*, 1986]. *Zwickl et al.* [1986] decomposed the distributions near the tail (in what is termed the intermediate ionized coma, or IIC) into three components: (1) a cold component with $T_e \approx 2 \times 10^4$ K and densities ranging

TABLE 4*b*. Ionization Frequencies per Electron for Impact Ionization of Atomic Oxygen by Maxwellian Electrons

Temp (K)	4S	2D	2P	Total
1.000E+04	4.579E-16	7.972E-18	2.310E-18	4.682E-16
2.000E+04	1.802E-12	2.170E-13	1.543E-13	2.173E-12
3.000E+04	3.410E-11	7.192E-12	6.865E-12	4.547E-11
4.000E+04	1.376E-10	4.332E-11	4.790E-11	2.288E-10
5.000E+04	3.435E-10	1.306E-10	1.577E-10	6.318E-10
6.000E+04	6.434E-10	2.771E-10	3.547E-10	1.275E-09
7.000E+04	1.020E-09	4.797E-10	6.403E-10	2.140E-09
8.000E+04	1.453E-09	7.300E-10	1.005E-09	3.188E-09
9.000E+04	1.926E-09	1.018E-09	1.436E-09	4.380E-09
1.000E+05	2.427E-09	1.336E-09	1.921E-09	5.684E-09
1.500E+05	5.035E-09	3.119E-09	4.750E-09	1.290E-08
2.000E+05	7.484E-09	4.910E-09	7.687E-09	2.008E-08
3.000E+05	1.154E-08	7.999E-09	1.287E-08	3.241E-08
4.000E+05	1.463E-08	1.041E-08	1.697E-08	4.201E-08
5.000E+05	1.703E-08	1.231E-08	2.021E-08	4.955E-08
6.000E+05	1.893E-08	1.382E-08	2.279E-08	5.554E-08
7.000E+05	2.049E-08	1.506E-08	2.492E-08	6.047E-08
8.000E+05	2.177E-08	1.608E-08	2.667E-08	6.452E-08
9.000E+05	2.284E-08	1.693E-08	2.814E-08	6.791E-08
1.000E+06	2.375E-08	1.765E-08	2.938E-08	7.078E-08
1.500E+06	2.667E-08	1.999E-08	3.340E-08	8.006E-08
2.000E+06	2.811E-08	2.115E-08	3.540E-08	8.466E-08
3.000E+06	2.911E-08	2.196E-08	3.682E-08	8.789E-08
4.000E+06	2.901E-08	2.193E-08	3.680E-08	8.774E-08
5.000E+06	2.850E-08	2.156E-08	3.619E-08	8.625E-08
7.000E+06	2.726E-08	2.064E-08	3.467E-08	8.257E-08
1.000E+07	2.544E-08	1.927E-08	3.238E-08	7.709E-08

Units of $cm^3\ s^{-1}$. Read 1.000E + 04 as 1.000×10^4. Rows refer to electron temperature, and columns refer to the ion final state. The total ionization frequency for a species is given in the last column.

from less than 10 cm^{-3} at $r \approx 10^4$ km to more than 200 cm^{-3} in the neutral sheet, (2) a midcomponent with $T_e \approx 2 \times 10^5$ K and $n_e \approx 20\ cm^{-3}$, (3) a hot component with $T_e \approx 8 \times 10^5$ K and $n_e \approx 0.3\ cm^{-3}$. Zwickl et al. notes that although the temperature of the midcomponent is comparable to solar wind temperatures, the density is considerably larger than even magnetosheath densities. They suggest that photoelectrons from photoionization of cometary neutrals are making an important contribution to the midcomponent. Cometary photoelectrons undoubtedly also make a contribution to the electron fluxes measured by VEGA below 70 eV (Figure 3*b*). The spatial volume where cometary photoelectrons make an important contribution to the overall electron distribution can be called the "plasma mantle" by analogy with the Venus plasma mantle [e.g., *Spenner et al.*, 1980]; this region appears to overlap approximately the cometary plasma region and its near-tailward extension.

The total H_2O and O ionization frequencies due to the VEGA electron distribution shown in Figure 3*b* were calculated using equation (4) and are listed in Table 5. R_{H_2O} and R_O values from this spectrum are quite large, approximately 4 times larger than the respective photoionization values. The ionization frequencies calculated from the 1-keV peak alone ($E > 800$ eV) are about half of the total. Again, the reader is reminded that due to possible errors in the spectrum, the derived ionization frequencies also have large uncertainties. The R_{H_2O} and R_O found by using Table 4 and a single effective temperature are more than 2 times greater than the "actual" values; but a single Maxwellian clearly cannot describe this spectrum. A three-component Maxwellian (see Table 5), although far from perfect, better represents the spectrum than a single-component Maxwellian; the resulting R_{H_2O} and R_O are then more satisfactory.

As mentioned above, cometary photoelectrons certainly make an important contribution to this spectrum for $E < 70$ eV; however, the large ionization frequency just from the 1-keV peak alone suggests that secondary electrons (see equation (4)) and even tertiary electrons also contribute to the spectrum and hence to the ionization frequency. The shape of the singly differential ionization cross section for H_2O versus secondary electron energy E_s is given by *Olivero et al.* [1972]. This shape is very similar for all species, as was shown by *Opal et al.* [1971]. The singly differential ionization cross section $S(E_s)$ at a given primary electron energy E is

$$S(E_s) = A/\{1 + (E_s/\mathbf{E}_s)^g\} \tag{7}$$

where $\mathbf{E}_s$ is typically about 8–10 eV and $g \approx 2$. The constant A is chosen such that the integral of $S(E_s)$ over E_s from 0 eV up to the maximum energy of a secondary electron, $E_{s\,max} = (E - I_s)/2$, gives the total ionization cross section for a pri-

TABLE 4c. Ionization Frequencies per Electron for Impact Ionization of Carbon Dioxide by Maxwellian Electrons

Temp. (K)	X	A	B	C	Dissoc.	Total
1.000E+04	9.665E-18	4.617E-18	2.508E-18	1.849E-19	6.989E-27	1.697E-17
2.000E+04	3.828E-13	2.171E-13	1.401E-13	2.169E-14	1.208E-17	7.617E-13
3.000E+04	1.470E-11	8.795E-12	5.991E-12	1.171E-12	1.573E-14	3.067E-11
4.000E+04	9.594E-11	5.880E-11	4.109E-11	8.941E-12	5.889E-13	2.054E-10
5.000E+04	3.040E-10	1.887E-10	1.338E-10	3.086E-11	5.289E-12	6.625E-10
6.000E+04	6.672E-10	4.174E-10	2.983E-10	7.126E-11	2.318E-11	1.477E-09
7.000E+04	1.183E-09	7.441E-10	5.349E-10	1.305E-10	6.731E-11	2.660E-09
8.000E+04	1.834E-09	1.158E-09	8.354E-10	2.066E-10	1.509E-10	4.185E-09
9.000E+04	2.593E-09	1.643E-09	1.189E-09	2.965E-10	2.845E-10	6.006E-09
1.000E+05	3.439E-09	2.185E-09	1.584E-09	3.971E-10	4.746E-10	8.080E-09
1.500E+05	8.316E-09	5.356E-09	3.898E-09	9.748E-10	2.288E-09	2.083E-08
2.000E+05	1.334E-08	8.717E-09	6.343E-09	1.559E-09	5.192E-09	3.515E-08
3.000E+05	2.215E-08	1.492E-08	1.084E-08	2.548E-09	1.223E-08	6.233E-08
4.000E+05	2.910E-08	2.018E-08	1.462E-08	3.307E-09	1.919E-08	8.640E-08
5.000E+05	3.456E-08	2.463E-08	1.781E-08	3.889E-09	2.540E-08	1.063E-07
6.000E+05	3.866E-08	2.840E-08	2.049E-08	4.347E-09	3.078E-08	1.229E-07
7.000E+05	4.234E-08	3.166E-08	2.281E-08	4.718E-09	3.537E-08	1.369E-07
8.000E+05	4.519E-08	3.449E-08	2.482E-08	5.018E-09	3.931E-08	1.488E-07
9.000E+05	4.753E-08	3.698E-08	2.658E-08	5.264E-09	4.269E-08	1.590E-07
1.000E+06	4.948E-08	3.918E-08	2.813E-08	5.470E-09	4.562E-08	1.679E-07
1.500E+06	5.544E-08	4.715E-08	3.374E-08	6.126E-09	5.543E-08	1.979E-07
2.000E+06	5.807E-08	5.214E-08	3.723E-08	6.442E-09	6.058E-08	2.145E-07
3.000E+06	5.936E-08	5.801E-08	4.130E-08	6.667E-09	6.474E-08	2.301E-07
4.000E+06	5.862E-08	6.114E-08	4.346E-08	6.673E-09	6.532E-08	2.352E-07
5.000E+06	5.716E-08	6.302E-08	4.474E-08	6.595E-09	6.470E-08	2.362E-07
7.000E+06	5.411E-08	6.453E-08	4.575E-08	6.377E-09	6.203E-08	2.328E-07
1.000E+07	5.000E-08	6.466E-08	4.576E-08	6.038E-09	5.828E-08	2.248E-07

Units of $cm^3\ s^{-1}$. Read 1.000E + 04 as 1.000×10^4. Rows refer to electron temperature, and columns refer to the ion final state. The total ionization frequency for a species is given in the last column.

mary electron energy E. Hence the electrons contributing to the spectrum at lower energies are probably a mixture of solar wind electrons, cometary photoelectrons, secondary electrons, and below 10 eV probably spacecraft photoelectrons. It is possible that a large part of it is in error due to contamination problems near closest approach.

Table 4 was used to find R_{H_2O} for each of the three components shown in Figure 2 of *Zwickl et al.* [1986] (see Figure 4). The cold component (with the highest density) made the least contribution to the total ionization frequency due to its low temperature. The contribution of the hot component to the total R_{H_2O} was rather modest due to the low density, even though the ionization rate per electron was large. The mid-component dominated the total ionization frequency. R_{H_2O} near the center of the tail (i.e., in the plasma sheet) is only about 50% of the photoionization rate, but somewhat farther out at a distance $\approx 10^4$ km from the tail axis, it is about the same as the photoionization rate. Recall that in the magnetosheath, R_{H_2O} was found to be about twice the photoionization rate; however, the electron parameters in the magnetosheath are highly variable so that R_s could easily be a factor of 2 or so, higher or lower, at any given UT [*Thomsen et al.*, 1986]. Secondary electrons no doubt make some contribution to the midcomponents and cold components and hence to the ionization frequency, but certainly they make much less of a contribution to the ICE distribution than to the Halley distribution because of the absence in the ICE distribution of a strong high-energy (≈ 1 keV) component.

7. Plasma Mantle: Electron Distributions in Cometary Plasma Region

The solar wind near Venus interacts rather "directly" with the ionosphere in that the ionosphere acts as a "hard" obstacle and diverts the solar wind around it [cf. *Russell and Vaisberg*, 1983; *Cloutier et al.*, 1983]. Actually, it is the magnetic barrier which diverts the bulk of the shocked solar wind around the planet, and there exists a sharp boundary (the ionopause) between the magnetized magnetosheath and the almost unmagnetized ionosphere. Thermal plasma pressure balances magnetic pressure at the ionopause surface. Mass loading of the magnetosheath flow does affect the flow behind the shock in that the pick up of neutrals ionized outside the ionopause contributes to the further stagnation of the flow and to the growth of the magnetic barrier and consequently also contributes to the development of the magnetotail [*Vaisberg and Zeleny*, 1984]. The extensive hot oxygen corona surrounding Venus [*Nagy et al.*, 1981; *Paxton*, 1983] contributes almost all of the heavy neutrals above the ionopause. The ionosphere becomes magnetized when the solar wind dynamic pressure is very large such that the plasma pressure in the ionosphere is insufficient to balance it.

The retarding potential analyzer (RPA) on the Pioneer

TABLE 4*d*. Ionization Frequencies per Electron for Impact Ionization of Carbon Monoxide by Maxwellian Electrons

Temp. (K)	X	A	B	Dissoc.	Total
1.000E+04	2.162E-16	1.599E-17	2.419E-19	1.986E-20	2.325E-16
2.000E+04	1.258E-12	3.642E-13	3.353E-14	1.061E-14	1.666E-12
3.000E+04	2.655E-11	1.176E-11	1.958E-12	9.789E-13	4.125E-11
4.000E+04	1.312E-10	7.135E-11	1.590E-11	1.006E-11	2.285E-10
5.000E+04	3.566E-10	2.188E-10	5.789E-11	4.247E-11	6.758E-10
6.000E+04	7.132E-10	4.738E-10	1.403E-10	1.140E-10	1.441E-09
7.000E+04	1.191E-09	8.371E-10	2.684E-10	2.355E-10	2.532E-09
8.000E+04	1.773E-09	1.299E-09	4.418E-10	4.117E-10	3.926E-09
9.000E+04	2.440E-09	1.847E-09	6.569E-10	6.426E-10	5.587E-09
1.000E+05	3.173E-09	2.464E-09	9.085E-10	9.254E-10	7.471E-09
1.500E+05	7.378E-09	6.183E-09	2.531E-09	2.943E-09	1.904E-08
2.000E+05	1.179E-08	1.024E-08	4.408E-09	5.529E-09	3.197E-08
3.000E+05	1.979E-08	1.783E-08	8.043E-09	1.098E-08	5.664E-08
4.000E+05	2.638E-08	2.416E-08	1.114E-08	1.590E-08	7.761E-08
5.000E+05	3.170E-08	2.932E-08	1.370E-08	2.015E-08	9.487E-08
6.000E+05	3.604E-08	3.354E-08	1.593E-08	2.369E-08	1.091E-07
7.000E+05	3.961E-08	3.702E-08	1.754E-08	2.666E-08	1.208E-07
8.000E+05	4.257E-08	3.992E-08	1.898E-08	2.916E-08	1.306E-07
9.000E+05	4.506E-08	4.235E-08	2.020E-08	3.126E-08	1.389E-07
1.000E+06	4.716E-08	4.441E-08	2.124E-08	3.303E-08	1.458E-07
1.500E+06	5.394E-08	5.107E-08	2.459E-08	3.872E-08	1.683E-07
2.000E+06	5.728E-08	5.435E-08	2.625E-08	4.137E-08	1.793E-07
3.000E+06	5.966E-08	5.672E-08	2.748E-08	4.281E-08	1.867E-07
4.000E+06	5.966E-08	5.681E-08	2.756E-08	4.224E-08	1.863E-07
5.000E+06	5.882E-08	5.604E-08	2.720E-08	4.092E-08	1.830E-07
7.000E+06	5.655E-08	5.392E-08	2.620E-08	3.822E-08	1.749E-07
1.000E+07	5.313E-08	5.067E-08	2.463E-08	3.456E-08	1.630E-07

Units of $cm^3\ s^{-1}$. Read 1.000E + 04 as 1.000×10^4. Rows refer to electron temperature, and columns refer to the ion final state. The total ionization frequency for a species is given in the last column.

Venus Orbiter (PVO) observed "superthermal" ($E >$ few eV) electrons both in the ionosphere and in the magnetosheath [*Spenner et al.*, 1980]. The electron distribution in a relatively narrow altitude region just outside the ionopause ($\Delta z \approx$ couple hundred kilometers in a layer roughly overlapping the inner part of the magnetic barrier) is no longer purely solar wind/magnetosheath but contains a photoelectron component which resembles the electron spectra measured in the ionosphere. *Spenner et al.* [1980] called this region the plasma mantle, and although it overlaps (not by accident) the stagnation/barrier region, it is defined by the nature of the electron distribution function. Both the electron spectrometers on Venera 9 and 10 [*Verigin et al.*, 1978] and the retarding potential analyzer on PVO observed these plasma mantle type distributions downstream of Venus in what was called the penumbra. It seems reasonable to assume that the photoelectrons in the mantle are generated near the dayside (where the neutrals are sufficiently dense), and then the photoelectrons flow downstream along field lines. Furthermore, electron fluxes were also observed in the umbra behind the planet and are the source of the weak Venusian aurora [cf. *Gringauz*, 1983].

By analogy with Venus, it makes sense to call the region near a comet, where the electron distributions contain both magnetosheath electrons and photoelectrons, the plasma mantle. Given the importance of electron impact ionization in the magnetosheath, one should also include secondary electrons as part of the "definition" of the plasma mantle electron distribution. Secondary electrons have relatively low energies like photoelectrons, but their spectra are less structured. The plasma mantle around comets is "fuzzier" than at Venus because the cometary neutral atmosphere is extremely extensive; hence photoelectrons are created over a huge volume. One can define the plasma mantle as that region where the photoelectron/secondary electron component of the total flux (designated PE) is comparable to the standard magnetosheath component. For comet G/Z the plasma mantle can be identified as the intermediate ionized coma discussed by *Zwickl et al.* 1986].

Just as for Venus, the plasma mantle roughly overlaps the stagnation/barrier region, or what *Gringauz et al.* [1986*a*, *b*] have called the cometary plasma region, which is a good term for this whole general region. We will now estimate the distance from the nucleus to the outer "boundary" of this region (r_{om}). The photoelectron/secondary electron number density is denoted n_{PE}. Due to the structure in the photoelectron part of the distribution, n_{PE} provides only a crude description of the distribution; n_{PE} is approximately

$$n_{PE} \approx R_s n_n \tau_{PE} \tag{8}$$

TABLE 4e. Ionization Frequencies per Electron for Impact Ionization of Molecular Nitrogen by Maxwellian Electrons

Temp. (K)	X	A	B	C	D	40 eV State	Total
1.000E+04	4.157E-17	5.672E-18	3.529E-19	1.387E-21	7.663E-21	2.275E-29	4.760E-17
2.000E+04	5.640E-13	1.460E-13	2.910E-14	1.834E-15	4.059E-15	4.396E-19	7.450E-13
3.000E+04	1.565E-11	4.987E-12	1.449E-12	2.251E-13	3.697E-13	1.225E-15	2.268E-11
4.000E+04	8.944E-11	3.151E-11	1.098E-11	2.640E-12	3.748E-12	6.714E-14	1.384E-10
5.000E+04	2.677E-10	9.989E-11	3.858E-11	1.196E-11	1.560E-11	7.569E-13	4.345E-10
6.000E+04	5.746E-10	2.224E-10	9.175E-11	3.349E-11	4.135E-11	3.853E-12	9.674E-10
7.000E+04	1.015E-09	4.025E-10	1.737E-10	7.096E-11	8.435E-11	1.242E-11	1.759E-09
8.000E+04	1.581E-09	6.381E-10	2.843E-10	1.260E-10	1.457E-10	3.007E-11	2.805E-09
9.000E+04	2.259E-09	9.238E-10	4.216E-10	1.987E-10	2.250E-10	6.006E-11	4.088E-09
1.000E+05	3.034E-09	1.253E-09	5.825E-10	2.879E-10	3.208E-10	1.048E-10	5.583E-09
1.500E+05	7.872E-09	3.338E-09	1.630E-09	9.185E-10	9.781E-10	5.701E-10	1.531E-08
2.000E+05	1.338E-08	5.738E-09	2.860E-09	1.705E-09	1.781E-09	1.354E-09	2.682E-08
3.000E+05	2.405E-08	1.040E-08	5.273E-09	3.301E-09	3.387E-09	3.279E-09	4.969E-08
4.000E+05	3.314E-08	1.438E-08	7.343E-09	4.691E-09	4.780E-09	5.157E-09	6.949E-08
5.000E+05	4.060E-08	1.765E-08	9.045E-09	5.841E-09	5.928E-09	6.790E-09	8.585E-08
6.000E+05	4.670E-08	2.032E-08	1.044E-08	6.782E-09	6.867E-09	8.172E-09	9.928E-08
7.000E+05	5.169E-08	2.252E-08	1.158E-08	7.559E-09	7.641E-09	9.325E-09	1.103E-08
8.000E+05	5.583E-08	2.433E-08	1.252E-08	8.201E-09	8.281E-09	1.029E-08	1.195E-07
9.000E+05	5.926E-08	2.583E-08	1.331E-08	8.735E-09	8.814E-09	1.111E-08	1.271E-07
1.000E+06	6.214E-08	2.710E-08	1.397E-08	9.184E-09	9.260E-09	1.179E-08	1.334E-07
1.500E+06	7.110E-08	3.103E-08	1.602E-08	1.059E-08	1.066E-08	1.401E-08	1.534E-07
2.000E+06	7.512E-08	3.280E-08	1.695E-08	1.124E-08	1.130E-08	1.508E-08	1.625E-07
3.000E+06	7.716E-08	3.371E-08	1.744E-08	1.160E-08	1.165E-08	1.580E-08	1.674E-07
4.000E+06	7.614E-08	3.328E-08	1.723E-08	1.148E-08	1.152E-08	1.574E-08	1.654E-07
5.000E+06	7.407E-08	3.238E-08	1.677E-08	1.119E-08	1.122E-08	1.545E-08	1.611E-07
7.000E+06	6.974E-08	3.050E-08	1.581E-08	1.057E-08	1.059E-08	1.461E-08	1.581E-07
1.000E+07	6.395E-08	2.797E-08	1.450E-08	9.706E-09	9.727E-09	1.358E-08	1.394E-07

Units of $cm^3\ s^{-1}$. Read 1.000E + 04 as 1.000×10^4. Rows refer to electron temperature, and columns refer to the ion final state. The total ionization frequency for a species is given in the last column.

where R_s is the ionization frequency (which is approximately $10^{-6}\ s^{-1}$ in the magnetosheath, about half from photoionization and half from impact ionization), n_n is the neutral density, and τ_{PE} is the lifetime of a photoelectron in the vicinity of the mantle.

The τ_{PE} is a sensitive function of several variables such as the electron energy (E), the neutral density, and the bulk flow speed or convection speed u; τ_{PE} is determined by transport processes far from the nucleus, where electron-neutral collisions are infrequent. Most photoelectrons have energies less than 30 eV or so, and typically photoelectron energies are about 10 eV. The average photoelectron with $E < 10$ eV is prevented from escaping from the general vicinity of the mantle/cometary plasma region along magnetic field lines by the polarization electric field. In this case, τ_{PE} is equal to the bulk plasma convection time, $\tau_{con} \approx r/u$, where r is the cometocentric distance and u is the flow velocity; r is an appropriate length scale. The flow speed for Halley is of the order of 1 km/s near 10^4 km [*Balsiger et al.*, 1986] and is about 50 km/s near 10^5 km [*Mukai et al.*, 1986]: u is about 50 km/s for $r \approx 10^4$ km at comet G/Z [*Bame et al.*, 1986]; $\tau_{con} \approx 2000$ s for Halley and 200 s for comet G/Z throughout most of the stagnation region, but τ_{con} increases to about 10^4 s near 10^4 km for comet Halley. Electrons of any origin with energies similar to magnetosheath electrons ($E > 20$ eV) will not be confined to the cometary plasma region by the polarization field and thus will have a residence time near the comet, τ_{PE}, much smaller than τ_{con}. Again, if one defines r_{om} as the distance where $n_{PE} \approx n_{SW} \approx 10\ cm^{-3}$ and then solves (6) for r, one finds that $r_{om} \approx 10^5$ km for Halley and $r_{om} \approx 5 \times 10^3$ to 10^4 km for comet G/Z. The spatial extent of the plasma mantle does indeed roughly correspond to the cometary plasma region [*Gringauz et al.*, 1986*a*, *b*].

Electron distributions in the cometary plasma mantle have several components: solar wind core (actually shocked solar wind core in the magnetosheath), solar wind halo, and photoelectron/secondary electrons. On the other hand, electron distributions in cometary ionospheres [e.g., *Mendis et al.*, 1985; *Marconi and Mendis*, 1986; *Boice et al.*, 1986; *Körösmezey et al.*, 1986] are expected to have two components: a cold dense component ($n_e \approx 10^3$–$10^4\ cm^{-3}$, $T_e \leq$ 1–2 eV) and a more energetic photoelectron component whose energy spectrum has considerable structure (*Körösmezey et al.*, 1986]. The analysis of thermal noise measured by the ICE radio experiment [*Meyer-Vernet et al.*, 1986] clearly demonstrated the existence of ionospheric type plasma ($n_e \approx 700\ cm^{-3}$, $T_e \approx 1.4 \times 10^4$ K) in the narrow confines of the plasma sheet of comet G/Z. *Zwickl et al.* [1986] observed a three-component plasma, the cold component of which persisted somewhat outside of the plasma sheet. *Zwickl et al.*'s [1986] interpretation was that the cold component must have been created closer to the nucleus and then convected downstream in the tailward direction be-

TABLE 4*f*. Ionization Frequencies per Electron for Impact Ionization of Atomic Hydrogen by Maxwellian Electrons

TEMP.	H Ionization
1.000E+04	1.900E-15
2.000E+04	4.240E-12
3.000E+04	6.190E-11
4.000E+04	2.490E-10
5.000E+04	5.930E-10
6.000E+04	1.080E-09
7.000E+04	1.670E-09
8.000E+04	2.340E-09
9.000E+04	3.060E-09
1.000E+05	3.820E-09
1.500E+05	7.640E-09
2.000E+05	1.110E-08
3.000E+05	1.650E-08
4.000E+05	2.050E-08
5.000E+05	2.330E-08
6.000E+05	2.540E-08
7.000E+05	2.690E-08
8.000E+05	2.810E-08
9.000E+05	2.890E-08
1.000E+06	2.950E-08
1.500E+06	3.030E-08
2.000E+06	2.950E-08
3.000E+06	2.670E-08
4.000E+06	2.410E-08
5.000E+06	2.200E-08
7.000E+06	1.880E-08
1.000E+07	1.560E-08

Units of $cm^3\ s^{-1}$. Read 1.000E + 04 as 1.000×10^4. Rows refer to electron temperature, and columns refer to the ion final state. The total ionization frequency for a species is given in the last column.

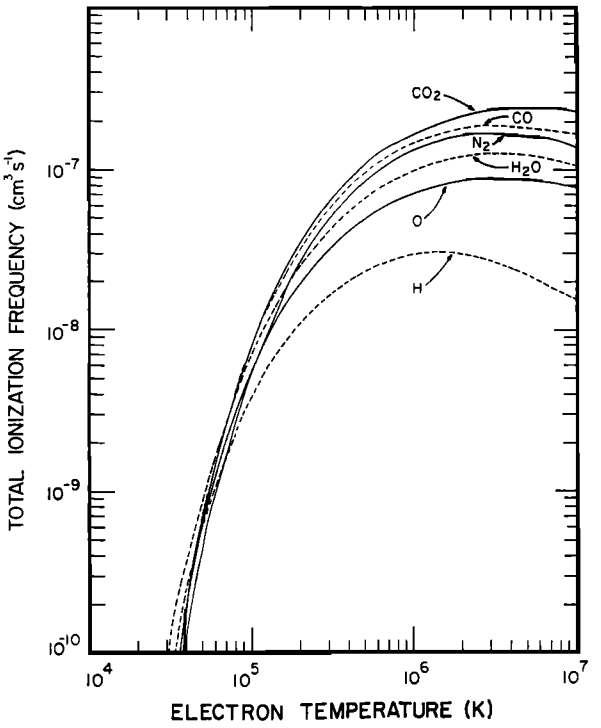

Fig. 2. Total normalized ionization frequencies (i.e., ionization frequency per incident electron) for several species as functions of electron temperature. The ionization frequency is obtained by multiplying these numbers by the electron density. To obtain the ionization rate requires a further multiplication by the relevant neutral number density. The electron distribution functions are assumed to be Maxwellian.

cause electron-neutral collisions in the vicinity of the ICE trajectory ($r \approx 10^4$ km) are quite infrequent. This seems to be a reasonable interpretation, and we will elaborate on this.

The inner part ($r \leq 1.5 \times 10^4$ km) of the cometary plasma region of comet Halley just outside the contact surface contains cold, dense, and slow moving plasma. Plasma instruments on Giotto [*Balsiger et al.*, 1986; *Krankowsky et al.*, 1986] measured densities comparable to ionospheric densities, ion temperatures of about 10^3K, and flow velocities about 1–2 km/s in this region. The bulk electron temperature, although not measured, is certainly rather low: the sum of the fitted components of the inner mantle distribution measured by *Gringauz et al.* [1986*a*] (Table 5) is less than 200 cm^{-3}, whereas theory indicates that n_e should be in excess of 10^3 cm^{-3} in this region [cf. *Cravens*, 1986*a*]. Consequently, T_e for the cold component must certainly be much less than ≈ 8 eV. This region, in which one has ionospheric-type plasma outside the classic ionosphere, could be given any of several names, such as the inner mantle, or inner cometary plasma region, or magnetized ionosphere [*Cravens*, 1986*a*]. The magnetometer experiment on Giotto [*Neubauer et al.*, 1986] indicated that the magnetic field strength drops to zero inside the contact surface which is located at $r \approx 4500$ km. The boundary between the inner plasma mantle (or inner cometary plasma region) and the outer cometary plasma region, r_{im}, can be defined as the outermost location where there is a "significant" density of cold (1–2 eV) electrons.

The photoelectron lifetime, in at least the outer part of the cometary plasma region, is determined primarily by transport processes, although some electron-neutral collisions are taking place in this region, as was shown in the earlier discussion on impact ionization. However, electron-neutral collisions become important and can modify the distribution function for r less than about $1–2 \times 10^4$ km (for comet Halley), even for unconfined electrons. The radial distance of this "electron collision zone" can be estimated by equating the electron-neutral collision time to the single-pass electron transit time $\tau \approx r/v_e$. The electron-neutral collision time is $\tau_{en} \approx 1/\{v_e \sigma n_n\}$, where v_e is the electron velocity and $\sigma \sim 2 \times 10^{-16}$ cm^2 is the total cross section. Ionization is not the only electron impact process operating: dissociation, electronic, and rotational excitation as well as general airglow processes are also possible [*Olivero et al.*, 1972; *Cravens and Green*, 1978; *Cravens and Körösmezey*, 1986; *Wallis and Ong*, 1975]. These inelastic processes can readily "cool" the electrons down to energies of about 5–15 eV, although it is more difficult to cool these electrons any further since electron energy loss processes are less effective for energies in the range 2–10 eV. Electron-electron Coulomb collisions are quite frequent for $E \approx 10$ eV and for $n_e \approx 10^3$ cm^{-3}, but these collisions will only smooth out the distribution and will not cool it unless there is a significant "seed" populations of cold electrons. Rotational and vibrational cooling due to neutral H_2O are the dominant

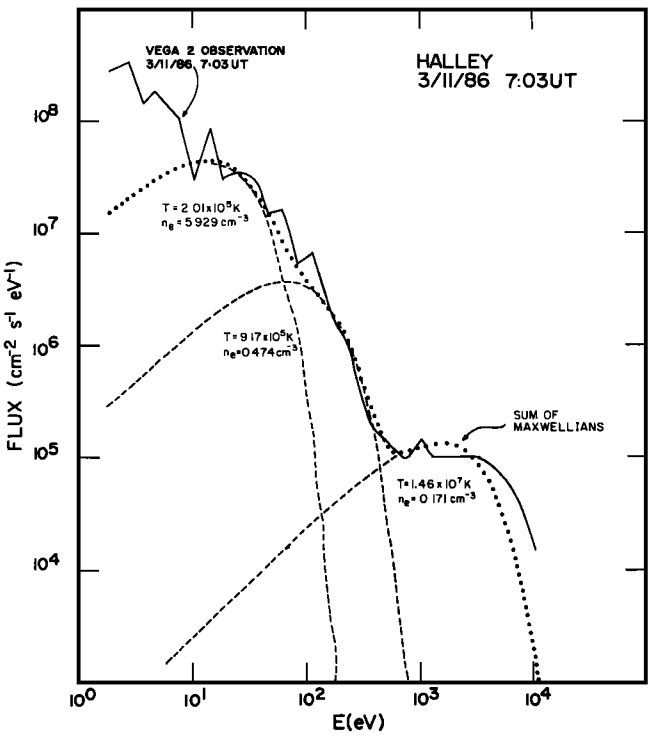

Fig. 3*a*. The solid line represents a published solar wind electron spectrum versus electron energy measured by the electron spectrometer on VEGA 2 [*Gringauz et al.*, 1986*a*].

TABLE 5. Ionization Frequencies R_{H_2O} and R_O From Measured Electron Spectra

Spectrum	Species H_2O	Species O
Comet G/Z		
0846 UT (solar wind)*	2.5×10^{-7}	1.9×10^{-7}
(5 cm^{-3}, 2.8×10^5 K)	(2.2×10^{-7})	(1.5×10^{-7})
1142 UT (magnetosheath)†	1.1×10^{-6}	8.3×10^{-7}
(20 cm^{-3}, 4×10^5 K)	(1.1×10^{-6})	(8.4×10^{-7})
1227 UT (solar wind)†	2.0×10^{-7}	1.6×10^{-7}
(8 cm^{-3}, 1.8×10^5 K)	(1.8×10^{-7})	(1.4×10^{-7})
Comet Halley		
0703 UT, March 11 (solar wind)‡	2.0×10^{-7}	1.5×10^{-7}
(10 cm^{-3}, 4.5×10^5 K)	(4.7×10^{-7})	(2.7×10^{-7})
(5.9 cm^{-3}, 2.00×10^5 K; 0.47 cm^{-3}, 9.2×10^5 K; 0.17 cm^{-3}, 1.5×10^7 K)	(2.1×10^{-7})	(1.6×10^{-7})
0713 UT, March 9 (mantle)‡	2.68×10^{-6}	1.99×10^{-6}
High-energy peak alone	1.58×10^{-6}	1.11×10^{-6}
(137 cm^{-3}, 4.2×10^5 K)	(8×10^{-6})	(6×10^{-6})
(50.2 cm^{-3}, 8.8×10^4 K; 28.3 cm^{-3}, 3.4×10^5 K; 10.1 cm^{-3}, 4.0×10^6 K)	(3.0×10^{-6})	(2.12×10^{-6})

Units of s^{-1}. The numbers in parentheses are the electron densities and effective electron temperatures for simple or multi-Maxwellian fits to the spectrum. The respective ionization frequencies were calculated using these parameters and Table 4.

**Bame et al.* [1986].

†*Thomsen et al.* [1986].

‡*Gringauz et al.* [1986*a*].

cooling processes for energies below about 10 eV. *Cravens and Körösmezey* [1986] calculated vibrational and rotational cooling rates for water. The total electron loss function for $E \approx 10$ eV is about $L \approx 3 \times 10^{-17}$ eV cm^2. Using this loss function gives a cooling time of $\tau_{cool} \approx E/\{v_e L\, n_n\} \approx 2 \times 10^9/n_n$; τ_{cool} is comparable to the transport time $\tau_{con} \approx 10^4$ s at $r_{im} \approx 1.5 \times 10^4$ km for comet Halley and at $r_{im} \approx 2 \times 10^3$ km for comet G/Z. A significant cold ($E < 1$–2eV) electron population should exist for r less than r_{im}.

Instruments on board Giotto [*Balsiger et al.*, 1986; *Krankowsky et al.*, 1986) observed a region of enhanced ion density somewhat outside the contact surface at a cometocentric distance of 1–2 $\times 10^4$ km. *Ip et al.* [1986] suggested that the ion pile up might be caused by a jump in the electron temperature which results in a reduced ion-electron recombination rate. Somewhat analogously, the cometary ionosphere models of *Körösmezey et al.* [1987] and *Marconi and Mendis* [1986] both predict plasma density enhancement where the electron temperature jumps. Hence it is suggestive that the location of the ion pile up region is approximately the same as the value of r_{im} estimated above.

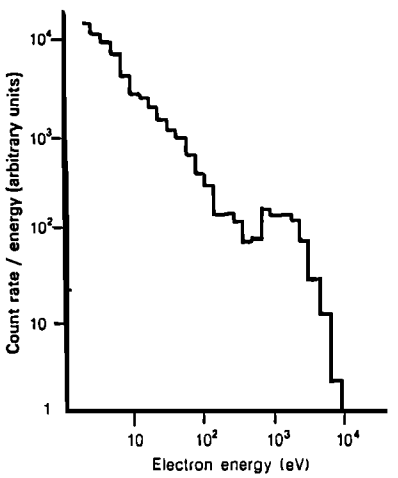

Fig. 3*b*. A published electron spectrum from a time near the closest approach of VEGA 2 to comet Halley is shown [*Gringauz et al.*, 1986*a*]. The omni-directional flux is plotted. A three-component Maxwellian fit to the measured spectrum is also shown.

In summary, the electron distribution in the inner mantle (or inner cometary plasma region) should have several components somewhat blended together: (1) a cold, dense component, (2) a photoelectron/secondary component, and (3) collision-modified solar wind core and halo components. In addition, in the VEGA data [*Gringauz et al.*, 1986*a*] there also appears to be an energetic ($\approx$0.5–1 keV) component, which seems to be more energetic than a typical solar wind halo distribution. Earlier in this paper it was shown that this energetic component contributes about half of the impact ionization rate.

8. Discussion

In this paper it was shown that the electron impact ionization rate in the unshocked solar wind is approximately 50% of the photoionization rate for solar minimum conditions. Charge exchange with solar wind protons is of approximately the same importance as photoionization; however, this process produces heavy ions but is not a source of electrons. For solar maximum the photoionization frequencies are 2–3 times larger, and electron impact ionization and charge exchange processes become relatively less important than during solar minimum conditions. The hotter and denser electron distributions which exist in the magnetosheaths of comets (or any planet for that matter) generate values of R_s which are about equal to, or somewhat larger than, photoionization fre-

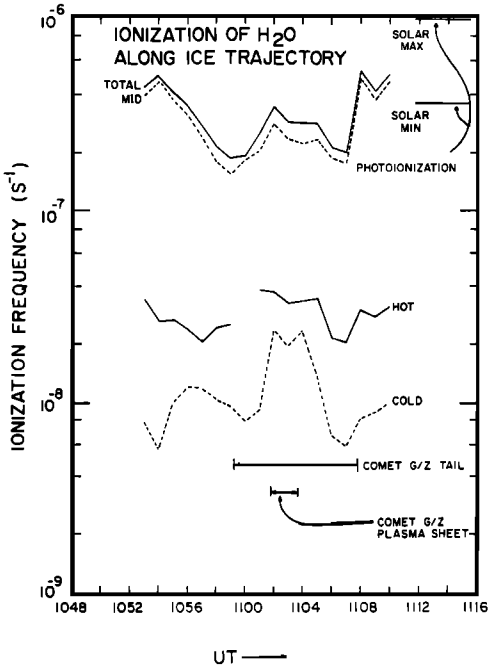

Fig. 4. The total ionization frequency of H_2O (leading to H_2O^+, OH^+, O^+, and H^+ but mostly H_2O^+) from electron impact is shown along a segment of the ICE spacecraft trajectory near its closest approach to comet Giacobini-Zinner. The three-component (cold, mid, and hot) electron densities and temperatures from *Zwickl et al.* [1986] (who used a three-component Maxwellian fit to match the observed electron spectra) were used together with the normalized ionization frequencies from Table 4 to calculate the ionization frequency for each component and the sum of the components. The widths of the magnetotail and plasma sheet of comet Giacobini-Zinner were taken from *Slavin et al.* [1986] and *Meyer-Vernet et al.* [1986].

quencies. Similarly, electron impact ionization in the near-tail region of comet G/Z is comparable in importance to photoionization. But closer to nucleus in the cometary plasma region of comet Halley, electron impact ionization is (possibly) much more important than photoionization, largely due to a high-energy peak in the observed electron flux. Clearly, numerical models of the interaction of the solar wind with comets should include this extra ionization source if the mass-loading rate is not to be underestimated.

It should be cautioned that the VEGA electron spectrum which was used to obtain this large ionization rate near closest approach is preliminary and might be in error. The electron impact ionization, which has been shown to take place throughout most of the magnetosheaths of comets Halley and Giacobini-Zinner, is basically due to electrons which have undergone "standard" heating in their passage through the bow shock; therefore this ionization source does not require any exotic or anomalous mechanism such as the Alfvén critical velocity mechanisms. The electron impact ionization frequency (or rate) in the inner cometary plasma region (or magnetized ionosphere), on the other hand, is very large and is, in large part, due to the high-energy peak. This high-energy peak contains too much flux, and the electrons are too energetic to be explained as a solar wind halo population, unless it were extremely modified. Hence the electron distribution and its resulting large ionization rate do require some further explanation (if they indeed really exist).

First, let us consider the possibility of the critical velocity mechanism [cf. *Formisano et al.*, 1982; *Galeev and Lipatov*, 1984]. The outer boundary of the anomalous ionization region calculated from equation (16) of *Galeev and Lipatov* [1984] is located near 10^4 km for a Halley-type comet. According to *Galeev and Lipatov* [1984] the heated electrons will have a temperature of the order of $T_e \approx M\,u^2/2$, where M is the mass of H_2O, CO_2, etc.; u is certainly no more than 10 km/s in this inner region (values more like 1 km/s were measured by Giotto, as discussed earlier), and this gives $T_e \approx 25$ eV for CO_2. This temperature is much less than the 0.5–1 keV energies of the electrons in the peak. Therefore the critical velocity mechanism appears to be an unlikely explanation for this energetic peak phenomena.

The possibility of an "internal" ionization source in excess of photoionization in the inner comas of comets was first considered by *Wurm* [1963] and *Wurm and Mammano* [1967], who observed the temporal and spatial structure of streamers in comet Morehouse and other comets. One explanation for this ionization effect was auroral-type precipitation requiring the discharge, or interruption, of the cross-tail current system [*Ip and Mendis*, 1976*a*, *b*] (also see reviews by *Ip and Axford* [1982] and *Mendis et al.* [1985]). The high-energy part of the spectrum measured by *Gringauz et al.* [1986*a*] in the inner cometary plasma region is indeed suggestive of terrestrial-type auroral spectra in inverted-V events. This possibility is also supported by the fact that the magnetic tail of comet Halley is well developed because the "hang up" time (same as the convection time used earlier) of the field lines in the inner plasma mantle or cometary plasma region is extremely long. This type of auroral activity is less likely to occur, or at least should be less vigorous, in comets like G/Z where the tail is less developed.

Acknowledgments. This work was supported by NASA grants NAGW-15 and NGR 23-005-015 and National Science Foundation grant ATM 8417884.

The Editor thanks A. E. S. Green and D. A. Mendis for their assistance in evaluating this paper.

REFERENCES

Alfvén, H., *On the Origin of the Solar System*, Oxford University Press, New York, 1954.

Balsiger, D. A., K. Altwegg, F. Bühler, J. Geiss, A. G. Ghielmetti, B. E. Goldstein, R. Goldstein, W. T. Huntress, W.-H. Ip, A. J. Lazarus, A. Meier, M. Neugebauer, U. Rettenmund, H. Rosenbauer, R. Schwenn, R. D. Sharp, E. G. Shelley, E. Ungstrup, and D. T. Young, Ion composition and dynamics at comet Halley, *Nature*, *321*, 330, 1986.

Bame, S. J., R. C. Anderson, J. R. Asbridge, D. N. Baker, W. C. Feldman, S. A. Fuselier, J. T. Gosling, D. J. McComas, M. F. Thomsen, D. T. Young, and R. D. Zwickl, Comet Giacobini-Zinner: Plasma description, *Science*, *232*, 356, 1986.

Banks, P. M., and G. Kockarts, *Aeronomy*, Academic, Orlando, Fla., 1973.

Boice, D. C., W. F. Huebner, J. J. Keady, H. U. Schmidt, and R. Wegmann, A model of comet P/Giacobini-Zinner, *Geophys. Res. Lett.*, *13*, 381, 1986.

Brandt, J. C., Observations and dynamics of plasma tails, in *Comets*, edited by L. L. Wilkening, p. 519, University of Arizona Press, Tucson, 1982.

Cloutier, P. A., T. F. Tascione, R. E. Daniell, Jr., H. A. Taylor, Jr., and R. S. Wolff, Physics of the interaction of the solar wind with Venus, in *Venus*, edited by D. M. Hunten, L. Colin, T. M. Donahue, and V. I. Moroz, p. 941, University of Arizona Press, Tucson, 1983.

Cravens, T. E., Theory and observations of cometary ionospheres, paper presented at COSPAR, Toulouse, France, 1986*a*.

Cravens, T. E., Ion distribution functions in the vicinity of comet Giacobini-Zinner, *Geophys. Res. Lett.*, *13*, 275, 1986*b*.

Cravens, T. E., and A. E. S. Green, Airglow from the inner comas of comets, *Icarus*, *33*, 612, 1978.

Cravens, T. E., and A. Körösmezey, Vibrational and rotational cooling of electrons by water vapor, *Planet. Space Sci., 34*, 961, 1986.

Feldman, W. C., J. R. Asbridge, S. J. Bame, M. D. Montgomery, and S. P. Gary, Solar wind electrons, *J. Geophys. Res., 80*, 4181, 1975.

Formisano, V., A. A. Galeev, and R. Z. Sagdeev, The role of the critical ionization velocity phenomena in the production of inner coma cometary plasma, *Planet. Space Sci., 30*, 491, 1982.

Galeev, A. A., and A. S. Lipatov, Plasma processes in cometary atmospheres, *Adv. Space Res., 4*, 229, 1984.

Galeev, A. A., T. E. Cravens, and T. I. Gombosi, Solar wind stagnation near comets, *Astrophys. J., 289*, 807, 1985.

Gloeckler, G., D. Hovestadt, F. M. Ipavich, M. Scholer, B. Klecker, and A. B. Calvin, Cometary pick-up ions observed near Giacobini-Zinner, *Geophys. Res. Lett., 13*, 251, 1986.

Gombosi, T. I., A. F. Nagy and T. E. Cravens, Dust and neutral gas modeling of the inner atmospheres of comets, *Rev. Geophys., 24*, 667, 1986.

Green, A. E.S., and R. S. Stolarski, Analytical models of electron impact excitation cross sections, *J. Atmos. Terr. Phys., 34*, 1703, 1972.

Gringauz, K. I., The bow shock and the magnetosphere of Venus according to measurements from Venera 9 and 10 orbiters, in *Venus*, edited by D. M. Hunten, L. Colin, T. M. Donahue, V. I. Moroz, p. 980, University of Arizona Press, Tucson, 1983.

Gringauz, K. I., T. I. Gombosi, A. P. Remizov, I. Apáthy, I. Szemerey, M. I. Verigin, L. I. Denchikova, A. V. Dyachkov, E. Keppler, I. N. Klimenko, A. K. Richter, A. J. Somogyi, K. Szego, S. Szendro, M. Tátrallyay, A. Varga, and G. A. Vladimirova, First in situ plasma and neutral gas measurements at comet Halley, *Nature, 321*, 282, 1986*a*.

Gringauz, K. I., T. I. Gombosi, M. Tátrallyay, M. I. Verigin, A. P. Remizov, A. K. Richter, I. Apáthy, I. Szemerey, A. V. Pyachkov, O. V. Balakina, and A. F. Nagy, Detection of a new "chemical" boundary at comet Halley, *Geophys. Res. Lett., 13*, 613, 1986*b*.

Haerendel, G., Plasma flow and critical velocity ionization in cometary comae, *Geophys. Res. Lett., 13*, 255, 1986.

Huebner, W. F., The photochemistry of comets, in *The Photochemistry of Atmospheres*, edited by J. S. Levine, p. 437, Academic, Orlando, Fla., 1985.

Hynds, R. J., S. W. H. Cowley, T. R. Sanderson, K. P. Wenzel, and J. J. VanRooijen, Observations of energetic ions from comet Giacobini-Zinner, *Science, 232*, 361, 1986.

Ip, W.-H., A preliminary consideration of the electron impact ionization effects in cometary comas, paper presented at Symposium 12, COSPAR, Toulouse, France, 1986.

Ip, W.-H., and W. I. Axford, Theories of physical processes in the cometary comae and ion tails, in *Comets*, edited by L. L. Wilkening, p. 588, University of Arizona Press, Tucson, 1982.

Ip, W.-H., and D. A. Mendis, Structure of cometary ionospheres, 1, H_2O-dominated comets, *Icarus, 28*, 389, 1976*a*.

Ip, W.-H., and D. A. Mendis, The generation of magnetic fields and electric currents in the cometary plasma tails, *Icarus, 29*, 147, 1976*b*.

Ip, W.-H., R. Schwenn, H. Rosenbauer, H. Balsiger, M. Neugebauer, and E. C. Shelley, An interpretation of the ion pile-up region outside the ionospheric contact surface, Proceedings of 20th ESLAB Symposium on the Exploration of Halley's Comet, Heidelberg, October 27–31, 1986, *Eur. Space Agency Spec. Publ., ESA SP-250*, 219, 1986.

Ipavich, F. M., A. B. Calvin, G. Gloeckler, D. Hovestadt, B. Klecker, and M. Scholer, Comet Giacobini-Zinner: In situ observations of energetic heavy ions, *Science, 232*, 366, 1986.

Jones, D. E., E. J. Smith, J. A. Slavin, B. T. Tsurutani, G. L. Siscoe, and D. A. Mendis, The bow wave of comet Giacobini-Zinner: ICE magnetic field observations, *Geophys. Res. Lett., 13*, 243, 1986.

Körösmezey, A., T. E. Cravens, T. I. Gombosi, A. F. Nagy, D. A. Mendis, K. Szego, B. E. Gribov, R. Z. Sagdeev, V. D. Shapiro, and V. I. Shevchenko, A new model of cometary ionospheres, *J. Geophys. Res.*, in press, 1987.

Krankowsky, D., P. Lämmerzahl, I. Herrwerth, J. Woweries, P. Eberhardt, U. Dolder, U. Herrmann, W. Schulte, J. J. Berthelier, J. M. Illiano, R. R. Hodges, and J. H. Hoffman, In situ gas and ion measurements at comet Halley, *Nature, 321*, 326, 1986.

Marconi, M. L., and D. A. Mendis, The electron density and temperature in the tail of comet Giacobini-Zinner, *Geophys. Res. Lett., 13*, 405, 1986.

McKenna-Lawlor, S., E. Kirsch, D. O'Sullivan, A. Thompson, and K. P. Wenzel, Energetic ions in the environment of comet Halley, *Nature, 321*, 347, 1986.

Mendis, D. A., H. L. F. Houpis, and M. L. Marconi, The physics of comets, *Fundam. Cosmic Phys., 10*, 1, 1985.

Meyer-Vernet, N., P. Couturier, S. Hoang, C. Perche, J. L. Steinberg, J. Fainberg, and C. Meetre, Plasma diagnosis from thermal noise and limits on dust flux or mass in comet P/Giacobini-Zinner, *Science, 232*, 370, 1986.

Mott, N. F., and H. S. W. Massey, *The Theory of Atomic Collisions*, Oxford University Press, New York, 1985.

Mukai, T., W. Miyake, T. Terasawa, M. Kitayama, and K. Hirao, Plasma observation by Suise of solar wind interaction with comet Halley, *Nature, 321*, 299, 1986.

Nagy, A. F., T. E. Cravens, J-H. Yee, and A. I. F. Stewart, Hot oxygen atoms in the upper atmosphere of Venus, *Geophys. Res. Lett., 8*, 629, 1981.

Neubauer, F. M., K. H. Glassmeier, M. Pohl, J. Raeder, M. H. Acuna, L. F. Burlaga, N. F. Ness, G. Musmann, F. Mariani, M. V. Wallis, E. Ungstrup, and H. U. Schmidt, First results from the Giotto magnetometer experiment at comet Halley, *Nature, 321*, 352, 1986.

Olivero, J. J., R. W. Stagat, and A. E. S. Green, Electron deposition in water vapor with atmospheric applications, *J. Geophys. Res., 77*, 4797, 1972.

Omidi, N., D. Winske, and C. S. Wu, The effect of heavy ions on the formation and structure of cometary bow shocks, *Icarus, 66*, 165, 1986.

Opal, C. B., W. K. Peterson, and E. C. Beaty, Secondary electron production cross sections, *J. Chem. Phys., 55*, 4100, 1971.

Paxton, L. J., Atomic carbon in the Venus thermosphere, Ph.D. dissertation, Univ. of Colo., Boulder, 1983.

Rème, H., J. A. Sauvaud, C. d'Uston, F. Cotin, A. Cros, K. A. Anderson, C. W. Carlson, D. W. Curtis, R. P. Lin, D. A. Mendis, A. Korth, and A. K. Richter, Comet Halley—Solar wind interaction from electron measurements aboard DGiotto, *Nature, 321*, 349, 1986.

Riedler, W., K. Schwingenschuh, Ye. G. Yeroshenko, V. A. Styashkin, and C. T. Russell, Magnetic field observations in comet Halley's coma, *Nature, 321*, 288, 1986.

Russell, C. T., and O. Vaisberg, The interaction of the solar wind with Venus, in *Venus*, edited by D. M. Hunten, L. Colin, T. M. Donahue, and V. I. Moroz, p. 873, University of Arizona Press, Tucson, 1983.

Sagdeev, R. Z., V. D. Shapiro, V. I. Shevchenko, and K. Szego, MHD turbulence in the solar wind—Comet interaction region, *Geophys. Res. Lett., 13*, 85, 1986.

Sawada, T, D. J. Strickland, and A. E. S. Green, Electron energy deposition in CO_2, *J. Geophys. Res., 77*, 4812, 1972*a*.

Sawada, T., D. L. Sellin, and A. E. S. Green, Electron impact excitation cross sections and energy degradation in CO, *J. Geophys. Res., 77*, 4819, 1972*b*.

Schmidt, H. U., and R. Wegmann, Plasma flow and magnetic fields in comets, in *Comets*, edited by L. L. Wilkening, p. 538, University of Arizona Press, Tucson, 1982.

Slavin, J. A., E. J. Smith, B. T. Tsurutani, G. L. Siscoe, D. E. Jones, and D. A. Mendis, Giacobini-Zinner magnetotail: ICE magnetic field observations, *Geophys. Res. Lett., 13*, 283, 1986.

Smith, E. J., B. T. Tsurutani, J. A. Slavin, D. E. Jones, G. L. Siscoe, and D. A. Mendis, International cometary explorer encounter with Giacobini-Zinner: Magnetic field observations, *Science, 232*, 382, 1986.

Somogyi, A. J., K. I. Gringauz, K. Szego, L. Szabó, Gy. Kozma, A. P. Remizov, J. Ero, Jr., I. N. Klimenko, I. T. Szücs, M. I. Verigin, J. Windberg, T. E. Cravens, A. Dyachkov, G. Erdos, M. Faragó, T. I. Gombosi, K. Kecskeméty, E. Keppler, T. Kovács, Jr., A. Kondor, Y. I. Logachev, L. Lohonyai, R. Marsden, R. Redl, A. K. Richter, V. G. Stolpovskii, J. Szabó, I. Szentpétery, A. Szepesváry, M. Tátrallyay, A. Varga, G. A. Vladimirova, K. P. Wenzel, and Z. Zarándy, First observations of energetic particles near comet Halley, *Nature, 321*, 285, 1986.

Spenner, K., W. C. Knudsen, K. L. Miller, V. Novak, C. T. Russell, and R. C. Elphic, Observation of the Venus mantle: The boundary region between solar wind and ionosphere, *J. Geophys. Res., 85*, 7655, 1980.

Stebbings, R. F., A. C. H. Smith, and H. Erhardt, Charge transfer between oxygen atoms and O^+ and H^+ ions, *J. Geophys. Res., 69*, 2349, 1964.

Tawara, H., Cross sections for charge transfer of hydrogen beams in gases and vapors in the energy range 10 eV–10 KeV, *At. Data Nucl. Data Tables, 22*, 491, 1978.

Thomsen, M. F., S. J. Bame, W. C. Feldman, J. T. Gosling, D. J. McComas, and D. T. Young, The comet/solar wind transition region at Giacobini-Zinner, *Geophys. Res. Lett., 13*, 393, 1986.

Torr, M. R., and D. G. Torr, Ionization frequencies for solar cycle 21: Revised, *J. Geophys. Res., 90*, 6675, 1985.

Tsurutani, B. T., and E. J. Smith, Strong hydromagnetic turbulence associated with comet Giacobini-Zinner, *Geophys. Res. Lett., 13*, 259, 1986.

Vaisberg, O. L., and L. M. Zeleny, Formation of the plasma mantle in the Venusian magnetosphere, *Icarus, 58*, 412, 1984.

Verigin, M. I., K. I. Gringauz, T. I. Gombosi, T. K. Breus, V. V. Bezrukikh, A. P. Remizov, and G. I. Volkov, Plasma near Venus from the Venera 9 and 10 wide-angle analyzer data, *J. Geophys. Res., 83*, 3721, 1978.

Wallis, M. K., Weakly shocked flows of the solar wind plasma through atmospheres of comets and planets, *Planet. Space Sci., 21*, 1647, 1973.

Wallis, M. K. and R. S. B. Ong, Strongly cooled ionizing plasma flows with application to beams, *Planet. Space Sci., 23*, 713, 1975.

Winske, D., C. S. Wu, Y. Y. Li, Z. Z. Mou, and S. Y. Guo, Coupling of newborn ions to the solar wind by electromagnetic instabilities and their interaction with the bow shock, *J. Geophys. Res., 90*, 2713, 1985.

Wurm, K., The physics of comets, in *The Solar System*, vol. 4, *The Moon, Meteorites and Comets*, edited by B. M. Middlehurst and G. P. Kuiper, p. 573, University of Chicago Press, Chicago, Ill., 1963.

Wurm, K., and A. Mammano, Dissociation and ionization in comets, *Icarus, 6*, 621, 1967.

Zwickl, R. D., D. N. Baker, S. J. Bame, W. C. Feldman, S. A. Fuselier, W. F. Huebner, D. J. McComas, and D. J. Young, Three component plasma electron distribution in the intermediate ionized coma of comet Giacobini-Zinner, *Geophys. Res. Lett., 13*, 401, 1986.

T. E. Cravens, T. I. Gombosi, J. U. Kozyra, M. Kurtz, and A. F. Nagy, Space Physics Research Laboratory, University of Michigan, 2455 Hayward, Ann Arbor, MI 48109.

(Received September 19, 1986;
revised March 10, 1987;
accepted November 13, 1986.)